Available online at www.eccomasproceedia.org
Eccomas Proceedia COMPDYN (2023) 648-676

ECCOMAS Proceedia

COMPDYN 2023
9th ECCOMAS Thematic Conference on
Computational Methods in Structural Dynamics and Earthquake Engineering
M. Papadrakakis, M. Fragiadakis (eds.)
Athens, Greece, 12-14 June 2023

THE SEISMIC PERFORMANCE OF THE DAMAGED BELL TOWER OF KOUROUKLATA IN KEFALONIA, GREECE DURING THE 2014 EARTHQUAKE SEQUENCE – A PROPOSAL FOR RETROFITTING

G.C. Manos[1], Lampros Kotoulas[1], Lazaros Melidis[1], Konstantinos Katakalos[1,2],

[1] Lab. Strength of Materials and Structures, Aristotle University, [2]Director
gcmanos@civil.auth.gr, lpkotoulas@gmail.com, lnmelidis@civil.auth.com,
kkatakal@civil.auth.gr

Abstract. *The dynamic and earthquake response of the bell tower of Ioannis Chrisostomos, located at the village of Kourouklata in the island of Kefalonia, Greece is examined here. This structure was subjected during the winter of 2014 in an intensive earthquake sequence, developing structural damage at the columns of its upper part. The 2014 strong earthquake sequence at the island of Kefalonia subjected a number of tall bell towers to considerable seismic forces. Despite the high amplitude of these seismic forces most bell towers in the island did not developed structural damage, with the exception of a bell tower located at the Kourouklata village. This bell tower is the subject of the current special study. The fact that the collapsed in 1953 earthquake sequence bell towers were masonry structures whereas the bell towers excited by the 2014 earthquake are reinforced concrete structures designed under the current seismic design provisions can explain the observed satisfactory earthquake performance. The dynamic and earthquake response of this bell tower was numerically simulated employing a 3-D elastic numerical simulation shell elements. The superstructure-foundation interaction was included in the numerical simulation. a third case is also examined whereby the stiffness of these links becomes even lower. The obtained numerical results of all these examined cases are presented and discussed. It is demonstrated that the soil – foundation – structure interaction influences the dynamic and earthquake response predictions for this structure quite significantly. Through all the presented results and the discussion the observed behaviour can be predicted reasonably well. The studied in this manuscript damaged Kourouklata bell tower revealed that the reinforced concrete structures built in Greece mainly after world war two and the enforcement of the New Code for Seismic Design, e.g. between 1950 and 1996, have a number of weaknesses that can lead to partial or total collapse. These weaknesses have been identified from some time by researchers and professionals specializing in earthquake engineering. Countermeasures for their strengthening are necessary. The effectiveness of such a retrofitting scheme employing pre-stressing cables is numerically studied here. The satisfactory performance of the Havriata bell tower studied previously demonstrates the effectiveness of the current design according to the provisions of the New Greek Seismic Code and Euro-Code8.*

Keywords: Bell towers, In-situ Dynamic Measurements, Numerical Simulation, Earthquake Response, Soil-structure Interaction.

Peer-review under responsibility of the organizing committee of COMPDYN 2023.
doi: 10.7712/120123.10426.20889

1. INTRODUCTION

Bell towers are structures that are of particular interest regarding their dynamic and earthquake response, which has been the subject of research in the past. A large number of bell towers with dimensions much larger than the ones examined here are located in numerous cities in Italy and elsewhere. The largest percentage of these bell towers is built by stone or brick masonry. In many cases earthquake activity constitutes the major cause of serious damage for bell towers that many times leads to partial or total collapse ([1] to [5]). Consequently, there is a major international concern for the stability of numerous bell towers. This resulted to significant international research effort that includes in-situ monitoring of the response of bell towers on a temporary basis, like the one attempted here, or more sophisticated and on a permanent basis ([6] to [13]). Foundation problems for bell towers are evident in many case the most celebrated being Pisa's grand bell tower in Italy, that is quoted as a major medieval engineering error. Therefore, the soil flexibility is also an area of research interest for these structures especially when their dynamic and earthquake response is under investigation ([20] to [24]).

The purpose of the current investigation is to study the seismic performance of a bell tower located at the village of Kourouklata in the island of Kefalonia, which is located in the most seismically active region of Greece. Whereas two new bell towers in Lixouri and in Havriata, which were studied before ([1] to [5]) were left undamaged this Kourouklata bell tower developed structural damage to its upper part.

2. EARTHQUAKE PERFORMANCE OF BELL TOWERS IN KEFALONIA

The island of Kefalonia, together with the nearby islands of Zakinthos, Leykatha and Ithaka (the birth place of the Homeric hero Ulysses), belongs to a seismic zone of Greece with the highest design ground acceleration equal to 0.36g, where g is the acceleration of gravity [18]. This is shown in figure 1 which depicts the seismic zoning map of Greece, together with the urban areas that were subjected to damaging earthquake sequences during the last 70 years that are in chronological order Argostoli (1953), Volos (1955), Thessaloniki (1978), Almiros (1980), Kalamata (1986), Pyrgos (1993), Kozani (1995), Aigio (1995), Athens (1999), Lixouri (2014). A description of the consequences of this earthquake activity is given by Manos [14] as well as by Papazachos and Papazachou [17]. A brief description of the consequences of the latest earthquake activity in the island of Kefalonia during 2014 together with considerable seismological and engineering information is included in the relevant report prepared under the auspices of the Earthquake Engineering Research Institute [15]. Furthermore, a numerical study of the seismic performance of Christian Churches that were damaged considerably by the 3rd of February 2014 Kefalonia earthquake is included in the work by Manos and coworkers [26] together with a study of a R/C structure as well as the Bell tower of Agios Gerasimos [1]. The reader is referred to these publications and only essential information is repeated here.

The earthquake of 1953 was of 7.3 Magnitude on the Richter scale and subjected to intense shaking the islands of Kefalonia, Ithaka and Zakinthos causing widespread destructions and human loss of 467 people. Following this earthquake a large number of people fled these islands, despite the recovery efforts. Argostoli, the capital city of Kefalonia, had the appearance of a heavily bombed city during World War II, as can be seen in figure 2. In comparison, figure 3 was taken before the 1953 earthquake. In this figure the location of a number of bell towers is also visible, indicated with red circles in order to facilitate the reader. It seems that the majority of these structures sustained considerable damage.

Figure 1. Seismic zoning map of Greece together with the urban areas that were damaged by earthquake activity during the last seventy (70) years. [18]

Figure 2. Total destruction of buildings during the Kefalonia 1953 earthquake.

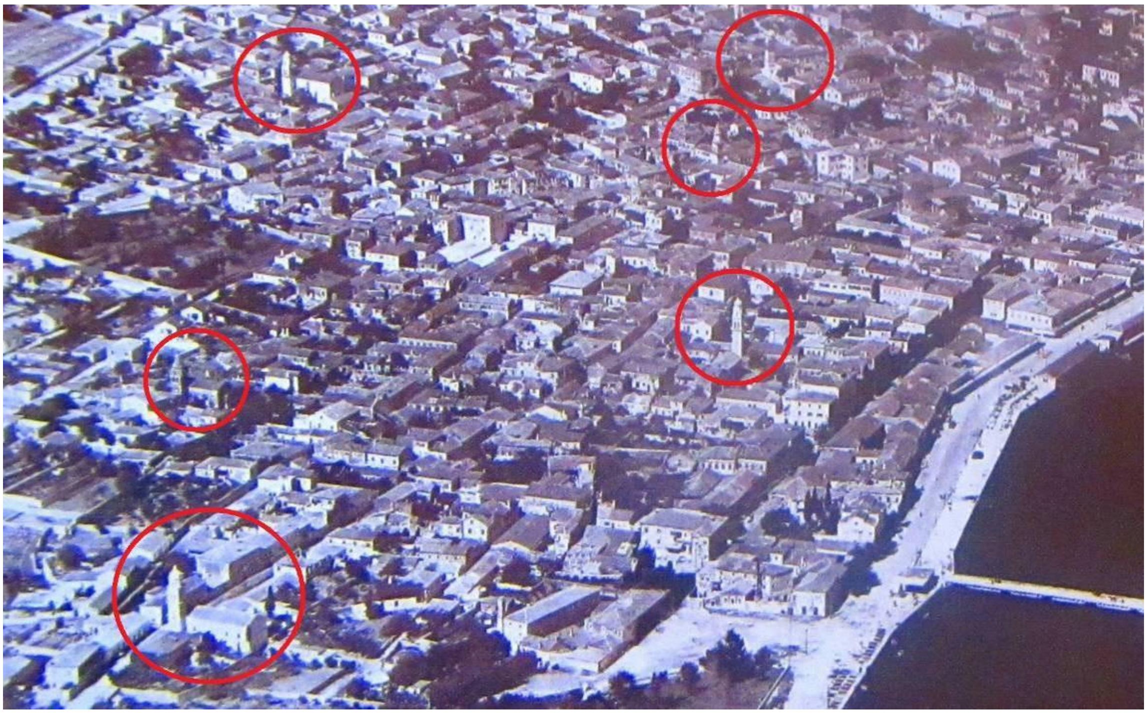

Figure 3. Areal view of Argostoli Kefalonia prior to the 1953 earthquake.

Figure 4. Stamp issued in 1953 by the Greek Post Organization

Figure 5. Partial collapse of the bell tower at the village of Kourouklata during the recent 2014 earthquake sequence

It is indicative that the Greek Post Organization issued that year two stamps one of which depicts the collapse of a bell tower, as is shown in figure 4. In line with this stamp is the partial collapse of the bell tower at the village of Kourouklata during the recent 2014 earthquake sequence, shown in figure 5. By comparing the damage depicted in this stamp and the Kourouklata bell tower damage an interesting observation can be made. The stamp bell tower failed by serious structural damage at a relatively lower level, presumably built with unreinforced masonry, whereas the Kourouklata bell tower damage is on the reinforced concrete (RC) columns of its upper part. This means that the Kourouklata bell tower was built after 1953 with the 1950 construction practices and materials for RC structures, which were proved to be insufficient as was the case for other types of RC structures [14].

3. NUMERICAL SIMULATION OF THE DYNAMIC RESPONSE OF THE ST. IOANNIS CHRISOSTOMOS BELL TOWER AT KOUROYKLATA

In the previous studies by Manos ([1] to [5]) the dynamic and earthquake response of the bell tower of Panayia Agriliotissa at Havriata was examined by numerically simulating its response in order to explain the observed performance. It was underlined, that this tower was built in 2009 (5 years before the recent earthquake sequence of 2014) well after the destructive earthquake of 1953 that caused the collapse of numerous bell towers in the island of Kefalonia. It was also underlined that this bell tower was designed taking into account the seismic load and seismic design provisions of the current provisions of the "New Greek Seismic" code. It was argued that this can partly explain the observed performance of this tower which was undamaged by this strong earthquake. Despite the fact that the details of the next studied bell tower in Lixouri (the bell tower of Agios Gerasimos [1] are not known in such depth the same rational can also be argued to be valid for this tower too. Both these towers were built with reinforced concrete and despite their considerable height did not exhibit any signs of distress either at the various parts of the superstructure or at their foundation. In the case of the bell tower at Havriata the structure of the nearby church of Panayia Agriliotissa [5] developed serious structural damage together with the retaining wall at the South part of this church are evidence of the intensity of this strong motion, being verified by the ground motion recordings. In the introduction, a number of bell towers were depicted located in various places in this island subjected to strong earthquake forces in 2014. Very few of them developed structural damage, which demonstrates the effectiveness of the adopted design and construction procedures since 1953. Based on experience from past earthquakes both in Greece as well as elsewhere the following represent a number of basic remarks, which are also shown in figures

A) Bell towers built with masonry and of considerable height are the most vulnerable. B) The attachment of the bell tower to the walls of the nearby church may have damaging effects. C) Many times, most vulnerable parts in a bell tower are the upper parts that are made weak by the openings as well as by the higher modes of vibration for these structures (cross-sections d-d and e-e in figure 1 as well as figures 6, 7, 8). D) Foundation settlements and poor maintenance can amplified the potential structural damage. In figure a) to d) the two studied towers of Agios Gerasimos at Lixouri and of Panayia Agriliotissa at Havriata are shown together with the tower of Agios Spyridon at Argostoli (not damaged) and the one at Agios Chrisostomos at Kourouklata with a particular type of damage that developed at its upper part (cross-section d-d). In what follows the type of numerical investigation, which was performed previously for the bell tower of Panagia Agriliotissa at Havriata, will be selectively performed in order to approximate the response of the bell tower of Agios Chrisostomos at Kourouklata (figure 5) in order to explain up to a degree the observed structural damage. Figures 6, 7, 8 depicts typical damage patterns.

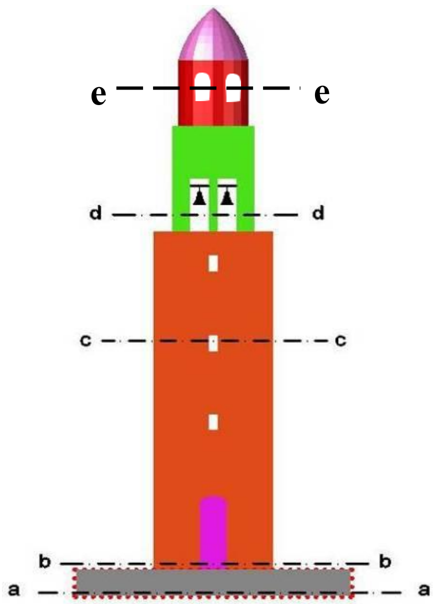

Figure 6. Schematic representation of a typical bell tower.

The three studied bell towers in Kefalonia island ([1] to [5]) have the following common parameters. A) Similar geometry. B) They are all detached from the nearby church structure. C) The upper part, which represents in most cases the most vulnerable part, is formed in two levels. The first part at cross-section formed by a series of columns d-d and the second at cross-section e-e which is also weakened by a series of openings.

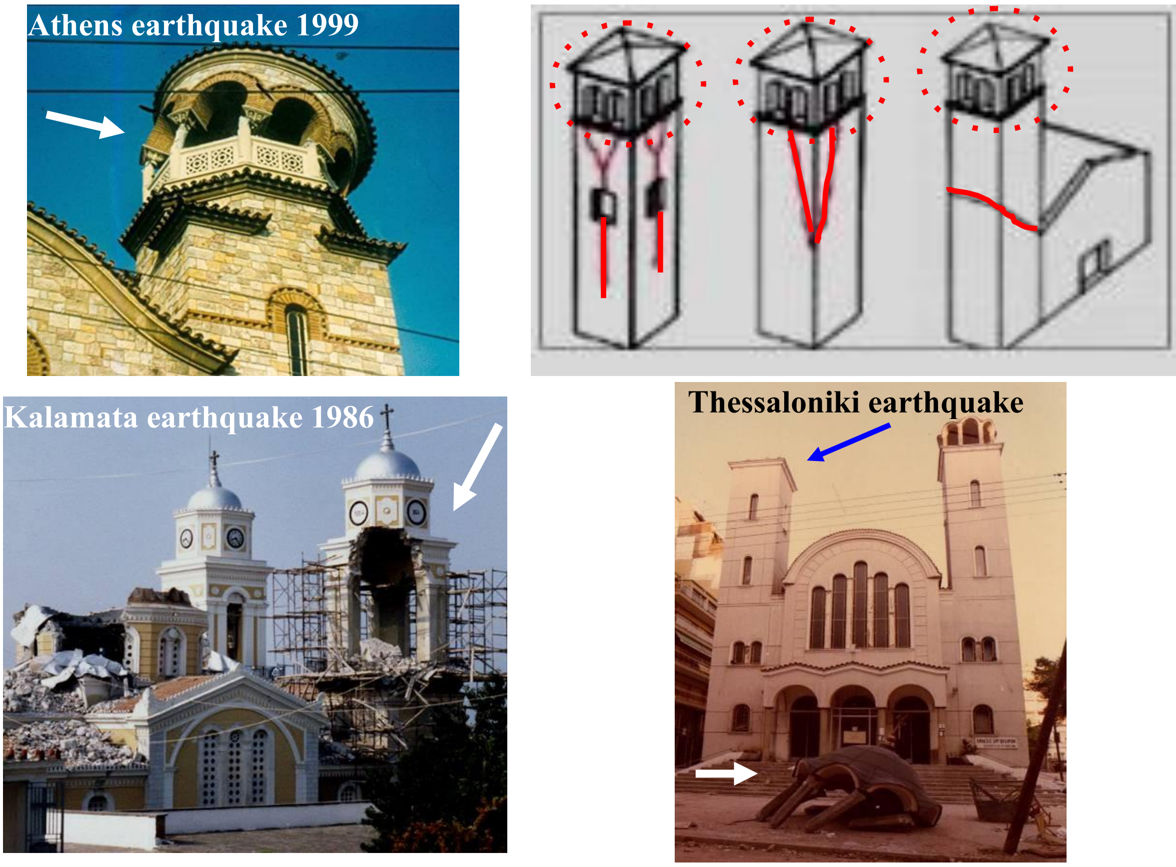

Figure 7. Typical earthquake damage patterns observed bell towers in Greece.

a) Ag. Gerasimos Lixouri 21.5m measured Detached.	b) Panagia, Havriata 21.5m measured Detached,	c) Ag. Spiridon Argostoli 14m estimated Detached,	j) Panayia Kourouklata 19m Estimated. Detached

Fig. 8. Studied bell towers in Kefalonia – Greece.

4. DYNAMIC SPECTRAL ANALYSIS

The numerical model used for the bell tower at Havriata [5] will be used again here with the following alterations. The part between cross-sections d-d and e-e is changed to represent the columns of the Kourouklata bell tower which as can be seen in figure 9 is much more flexible than the corresponding part of the Havriata bell tower. This is clearly seen in figure where the Kourouklata bell tower is depicted as it stood prior to being damaged by the 2014 earthquake. It must be underlined that both this bell tower as well the nearby church were built new after the 1953 destructive earthquake. In reference (EERI [15]) reports deformations of the soil terrain at the vicinity of this bell tower, which is built on a hill. Moreover, severe damage is reported on the gravestones of the cemetery of this church which is close to the bell tower thus indicating the intensity of the earthquake ground motion. In contrast to the bell towers of Agios Gerasimos at Lixouri and the bell tower at Havriata, whereby the earthquake ground motion was recorded by an instrument located only 100meters from each bell tower there was not such recording for the bell tower at Kourouklata ([15] and [16]).

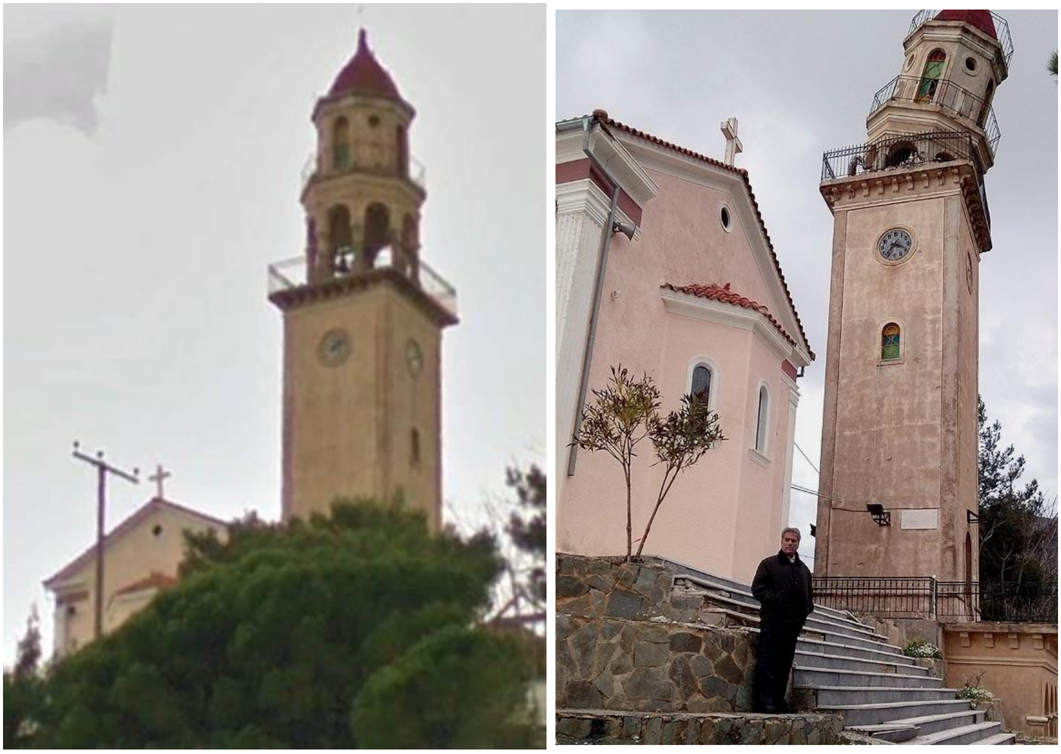

Figure 9. The bell tower at Kourouklata priot and after the earthquake sequence of 2014.

This bell tower is placed at a distance of about 9klm from the epicenters of both the strongest aftershock (3rd February 2014) which caused widespread damage and according to witness reports caused the collapse of this bell tower at Kourouklata. It is not known whether the main event initiated this structural damage. The location of these three bell towers together with the location of the epicenters and the location of the instruments which recorded the ground motion records for either the main event or this strongest aftershock are shown in figure 10. It can be seen that Kourouklata bell tower is located at a distance of approximately 5km from either Argostoli or Lixouri, where the ground motion was recorded. Moreover, the distance of the Kourouklata bell tower from the epicenter is approximately 9km whereas the distance of the Agios Gerasimos bell tower at Lixouri and the Panaya

Agriliotissa bell tower at Havriata from the epicenter is approximately 6km and 4km, respectively. At this stage no attempt is made to introduce any attenuation relationships or to take into account the site-effects, which may have played an important role for the case of the bell tower at Kourouklata [15]. At present, the strong motion recorded at Lixouri during the 3rd of February aftershock is assumed as input in the subsequent numerical analysis.

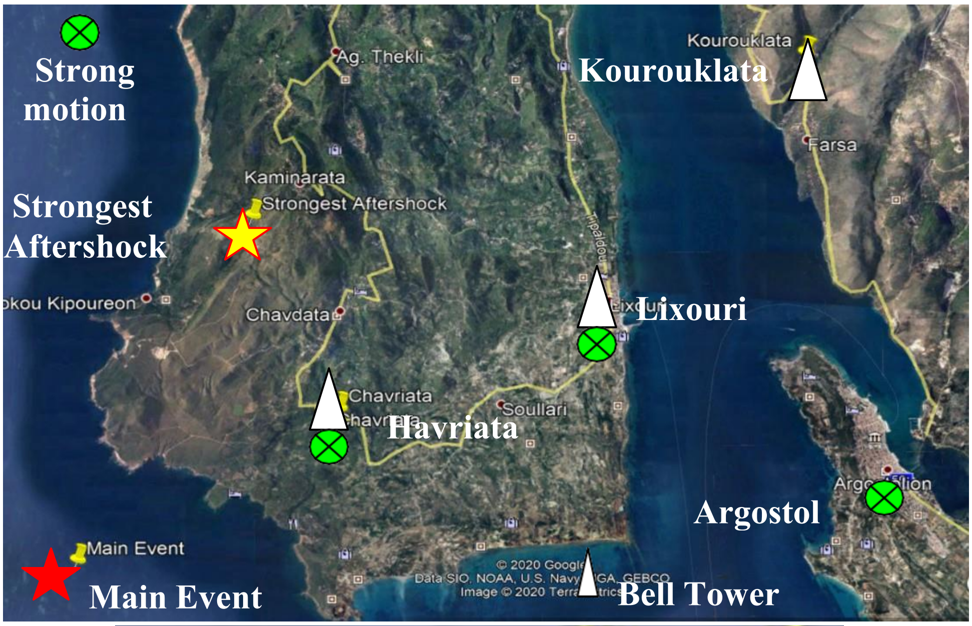

Figure 10. The location of the epicenters, the bell towers and the instruments that recorded the earthquake strong ground motion

In figure 11 the total destruction of one of the columns of this upper part of the Kourouklata bell tower is shown. As can be seen the earthquake forces caused the total disintegration of the largest part of these columns. Moreover, at this stage an absence of closed stirrups may be deduced from this figure. At the right side of this figure the removal of this damaged upper part is shown. From a concrete sample taken from these columns a compressive stress equal to 21MPa was found. In figures 12 the numerical simulation of this bell tower is shown together with the most significant eigen-modes. The values of the corresponding eigen-periods and modal mass participation ratios (Mi) are also included. These values are also listed in table 1. Table 1 lists the values of the base shear and the overturning moment resulting from all the elastic numerical analyses.

Figure 11. The damaged columns of the upper part of the Kourouklata bell tower

TABLE 1: Modal Participating Mass Ratios

		Period	UX	UY	UZ	SumUX	SumUY	SumUZ
		Sec	Unitless	Unitless	Unitless	Unitless	Unitless	Unitless
Mode	1	0,251		0,307			0,307	
Mode	2	0,249	0,309			0,310	0,307	
Mode	3	0,128				0,310	0,308	
Mode	4	0,107	0,401			0,711	0,308	
Mode	5	0,106		0,384		0,711	0,692	
Mode	6	0,061				0,711	0,693	
Mode	7	0,061				0,711	0,693	
Mode	8	0,050				0,712	0,693	
Mode	9	0,049			0,335	0,712	0,693	0,335
Mode	10	0,036	0,158			0,870	0,693	0,335
Mode	11	0,034		0,168		0,871	0,861	0,335
Mode	12	0,032				0,871	0,861	0,335

Figure 12 depicts the undeformed Kourouklata bell tower and the four (4) most dominant eigen-modes as they were predicted through the adopted numerical simulation. As it is noted in this figure the 1st and 2nd eigen-modes with 0.304sec eigen-period mobilize 15.8% of the total mass of this bell-tower. In addition, the 4th and 5th eigen-modes with 0.116sec eigen-period mobilize 46.0% of the total mass of this bell-tower. Therefore, these four eigen-modes mobilize nearly 70% in either the North-South (x-x) and/or the East-West (y-y) directions respectively. This can also be seen in Table for both the 1st and 2nd (North-South and East-West) as well as the 4th and 5th (North-South and East-West) translational eigen-modes for this bell tower. Moreover, the presence of this relatively "soft" story at the level where the bells are located influences the resulting dynamic response of this structure in a significant way, as can be seen in figures 12. Table 2 lists the values of the base shear and overturning moment for all the linear elastic analyses that were performed at this stage.

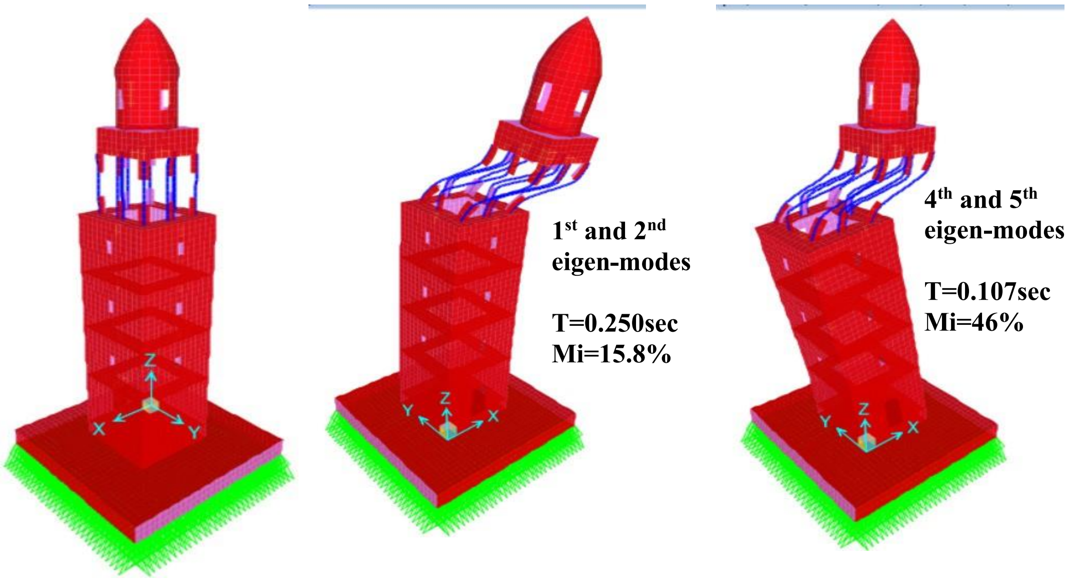

Figure 12. Numerical simulation of the bell tower at Kourouklata - the most significant eigen-modes

Table 2. Base reactions from the performed numerical analyses for this bell tower

			GlobalFX	GlobalFY	GlobalFZ	GlobalMX	GlobalMY
			Tonf	Tonf	Tonf	Tonf-m	Tonf-m
DEAD	LinStatic				**518***		
ResSpec EW Lin 05	LinRespSpec	Max		**94**		**1075**	
ResSpec NS Lin 05	LinRespSpec	Max	**89**				**903**
ResSpec NS NonLin m3	LinRespSpec	Max		**70**		**741**	
ResSpec EW NonLin m3	LinRespSpec	Max	**60**				**592**
Lix Time EW	LinDirHist	Max		**91**		**1529**	
Lix Time EW	LinDirHist	Min		**-175**		**-783**	
Lix Time NS	LinDirHist	Max	**118**				**860**
Lix Time NS	LinDirHist	Min	**-115**				**-1124**
COMB2	Combination	Max	**27**	**94**	**519**	**1078**	**272**
COMB2	Combination	Min	**-27**	**-94**	**517**	**-1073**	**-272**
COMB3	Combination	Max	**89**	**28**	**519**	**326**	**903**
COMB3	Combination	Min	**-89**	**-28**	**518**	**-321**	**-904**
COMB4	Combination	Max	**60**	**21**	**519**	**226**	**592**
COMB4	Combination	Min	**-60**	**-21**	**518**	**-220**	**-593**
COMB5	Combination	Max	**18**	**70**	**519**	**744**	**178**
COMB5	Combination	Min	**-18**	**-70**	**517**	**-738**	**-179**

* The weight of the superstructure (without the foundation block) is 208tnf

COMB2 = DEAD + ResSpecEW-05 + 0.3ResSpecNS-05
COMB3 = DEAD + 0.3ResSpecEW-05 + ResSpecNS-05
COMB4 = DEAD + 0.3ResSpecEW-NonLin m3 + ResSpecNS-NonLin m3
COMB5 = DEAD + ResSpecEW-NonLin m3 + ResSpecNS-NonLin m3

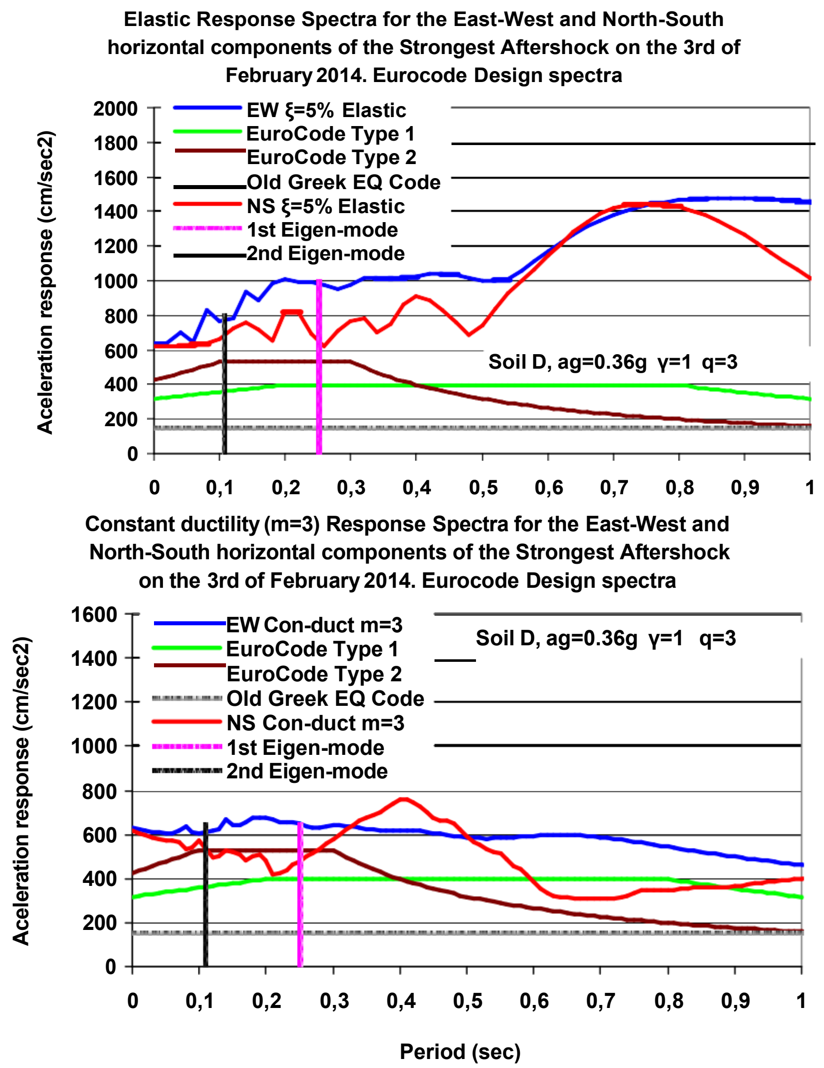

Figure 13. design acceleration spectral curves as well as the constant ductility spectral curves derived from the ground seismic motion recorded at Lixouri and were used for the dynamic spectral analyses

Table 3. Extreme stress resultant for the columns supporting the bells

Table Maximum / minimum values of shear force or bending moment values	Axial (KN)	Q2-2 (KN)	Q3-3 (KN)	M2-2 (KNm)	M3-3 (KNm)
COMB2 = DEAD + ResSpecEW-05 + 0.3ResSpecNS-05	**172 / -270**		**73 / -76**	**44 / -42**	
COMB3 = DEAD + 0.3ResSpecEW-05 + ResSpecNS-05	**158 / -257**	**56 / -60**			**37 / -35**
COMB4 = DEAD + 0.3ResSpecEW-NonLin m3 + ResSpecNS-NonLin m3	**87 / -184**	**36 / -40**			**24 / -23**
COMB5 = DEAD + ResSpecEW-NonLin m3 + 0.3ResSpecNS-NonLin m3	**97 / -196**		**48 / -52**	**25 / - 28**	

Figure 13 depicts the design acceleration spectral curves as well as the constant ductility spectral curves derived from the ground seismic motion recorded at Lixouri and were used for the dynamic spectral analyses. Table 3 lists the maximum / minimum values of the axial / shear forces or bending moments that develop at the columns of the upper part of the Kouraklata bell tower, which failed during the 2014 earthquake, as they were obtained for the dynamic spectral analyses using the load combinations listed in this table.

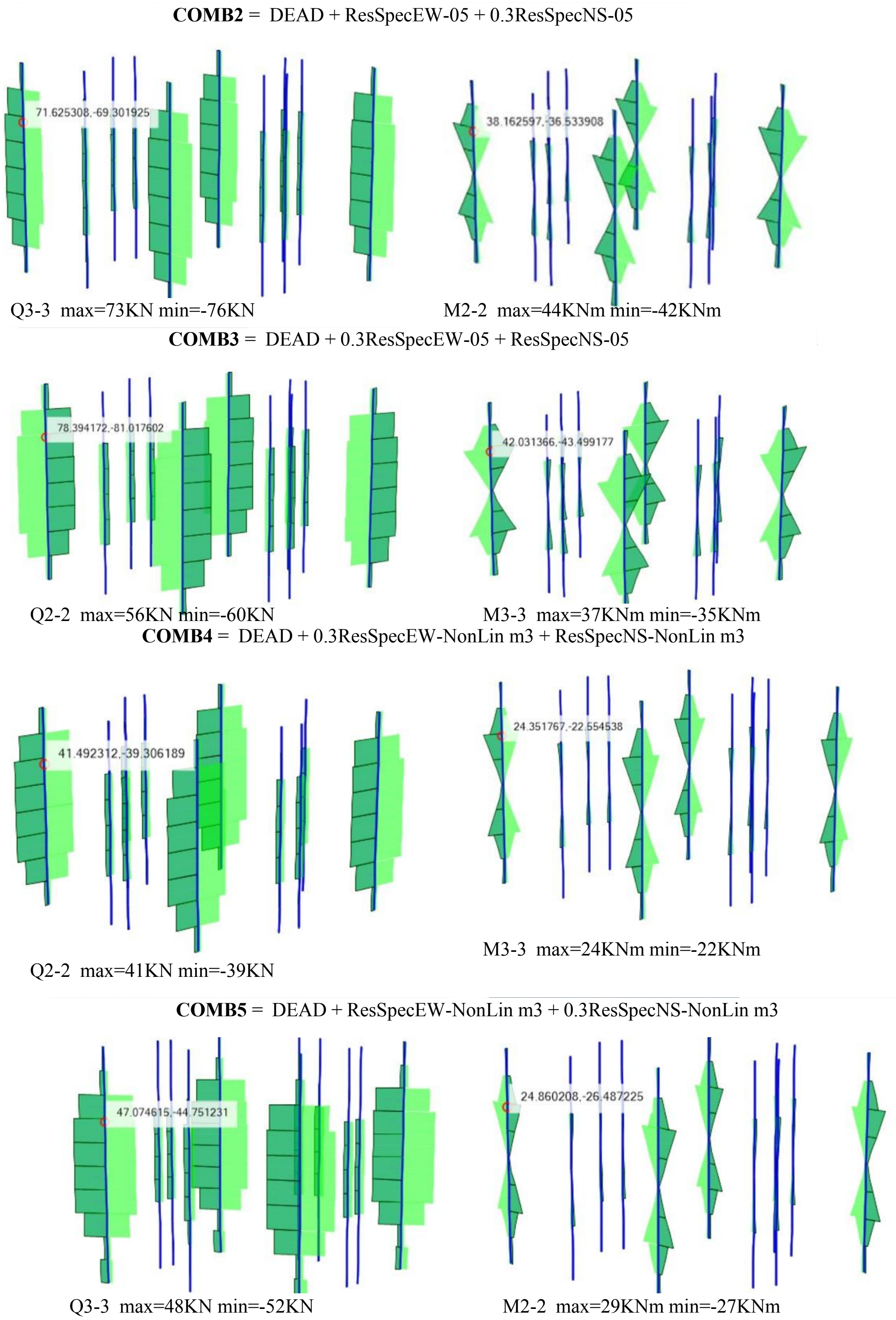

Figure 14. Distribution of shear forces and bending moment along the height of the columns supporting the upper part of the bell tower at Kourouklata for all load combinations

Figure 14 depicts these columns and the distribution of the shear force and bending moment diagrams over the height of the failed columns as predicted for the various combinations through the adopted numerical analysis. As can be seen, the values resulting when the elastic-response spectra are used are twice as much as the values when a non-linear response spectra curves are used with a ductility coefficient m=3. Judging from the failure mode of these columns a ductility value equal to 3 seems non-conservative. As can be seen these later reduced capacity values are smaller than the demands predicted to occur for load combinations COMB2 and COMB3 (linear response spectra) and about the same level as the demands predicted for load combinations COMB4 and COMB5 (non-linear response spectra for ductility coefficient m=3). Table 4 lists the shear and flexural capacities for three different levels of axial force, zero (0KN) compression of 200KN and tension of 100KN. The cross-section of each column is 300mm x 300mm and the longitudinal reinforcement comprises of eight (8) reinforcing bars having a diameter of 14mm each and a yield stress of 240MPa. As transverse reinforcement steel stirrups of a diameter of 6mm spaced every 500mm are considered. The compressive strength of the concrete was found from an axial compression tests performed on a cube with a cross section 36.0mm x 31.0mm and a height of 36.5mm sampled from the base of one of these columns at Kourouklata and tested at the Laboratory of Strength of Materials and Structures of Aristotle University after being formed and cupped, as shown in figure 15. The steel properties were assumed to be valid for the category of steel reinforcing bars of this type used in Greece for this period of construction.

Table 4. Shear and flexural capacities of the columns supporting the bells at the upper part of the bell tower

.	Axial force level (KN)	Shear force (KN)	Bending Moment (KNm)
**** Capacities for axial force 0KN***	**0**	**77**	**38.6**
**** Capacities for axial force 200KN compression***	**-200**	**103**	**60.8**
**** Capacities for axial force 100KN tesnion***	**100**	**64**	**27.3**

- Column cross-section 300mm x 300mm, fc=21.2MPa, 8 rebars 14mm diameter each, fy=240MPa.
-

Fig. 15. Compressive test of a concrete sample taken from the bell tower columns (fc=21.2MPa)

Table 5 lists the ratios values of the demands over the corresponding capacity values (listed in table 4) for the extreme stress resultant for the columns supporting the bells listed in table 3. The above demand / capacity comparison can partly explain the observed failure of these columns. As already discussed, the formation of the “soft” story by these slender non-ductile columns at this level must be considered as the fundamental earthquake damage generating mechanism for this bell tower.

Table 5. Ratios* of demands / capacity values for the extreme stress resultant for the columns supporting the bells

	Level of Axial Force (KN)	Ratio Q2-2	Ratio Q3-3	Ratio M2-2	Ratio M3-3
COMB2 = DEAD + ResSpecEW-05 + 0.3ResSpecNS-05	**172 / -270**		**1.14 * / 0.74**	**1.61 * / 0.69**	
COMB3 = DEAD + 0.3ResSpecEW-05 + ResSpecNS-05	**158 / -257**	**0.88 / 0.58**			**1.36 * / 0.58**
COMB4 = DEAD + 0.3ResSpecEW-NonLin m3 + ResSpecNS-NonLin m3	**87 / -184**	**0.56 / 0.39**			**0.88 / 0.38**
COMB5 = DEAD + ResSpecEW-NonLin m3 + 0.3ResSpecNS-NonLin m3	**97 / -196**		**0.75 / 0.50**	**0.92 / 0.46**	

* Ratio values larger than one indicate structural damage

Figure 16 depicts the deformed shape of this bell tower when subjecting to these four (4) load combinations highlighting again the significance of this earthquake damage generating mechanism. This earthquake damage generating mechanism is a common feature for many existing bell-towers constructed with relatively "old" earthquake design provisions, even if they are built with reinforced concrete structural elements, as was the case for the bell tower at Kourouklata. As was shown, the earthquake force levels require structural elements that are equipped with a considerable percentage of longitudinal and transverse reinforcement and a high quality concrete so that they can sustain the high shear force and bending moment demands posed on them by a strong earthquake motion having at the same time the ability to perform in a ductile behaviour, as was the case of the bell tower at Havriata [5].

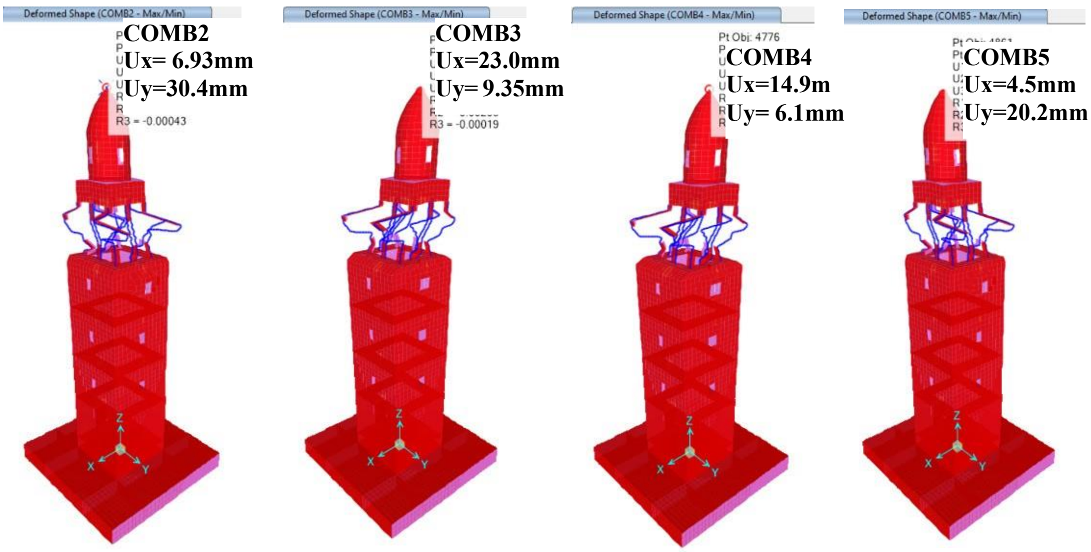

Figure 16. The maximum horizontal displacement response at the top of the Kourouklata bell tower for the four load combinations listed at table .

5. TIME HISTORY NUMERICAL ANALYSES.

In this section the results of a series of numerical predictions of the Kourouklata bell tower are presented and discussed. The same numerical simulation used in the previous section is used again here. However, step-by-step time history analyses are performed employing the two horizontal components of the ground motion recorded at Lixouri during the 3rd of February 2014. In what follows response predictions employing the East-West horizontal component of the recorded earthquake ground motion are shown. For the non-linear time history analysis all the vertical supports of the foundation block were provided with a non-linear constitutive behaviour that could sustain very little tension and a non-linear compression path as the one shown in figure 17. However, the unloading path was not following this multi-linear behaviour shown in this figure, Instead, this time the development of plastic deformations at each un-loading level was adopted. Moreover, the system of horizontal forces used this time comprise by a pair of horizontal forces applied at the corners of the bell tower at a height of 12.88m from the base of the tower. This non-linear behaviour of the vertical supports of the foundation block attempt to simulate the possibility of the foundation block to uplift from the underlying soil layers when tensile forces develop at this interface.

Moreover, the non-linear behaviour of these soil-layers in compression is also approximated. This behaviour must of course be validated from data to be obtained from an in-depth study of the dynamic properties of these underlying soil layers which is beyond the scope of the current study.

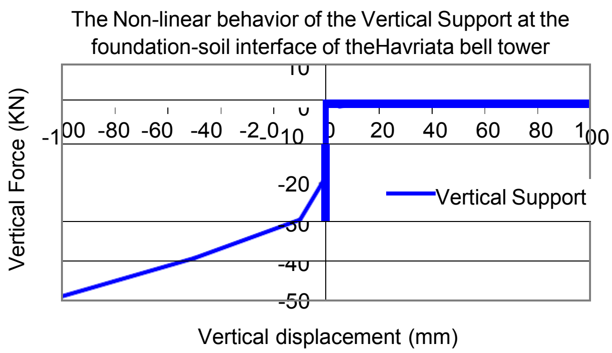

Fig. 17. The non-linear constitutive behaviour of the vertical links supporting the foundation block of the bell tower.

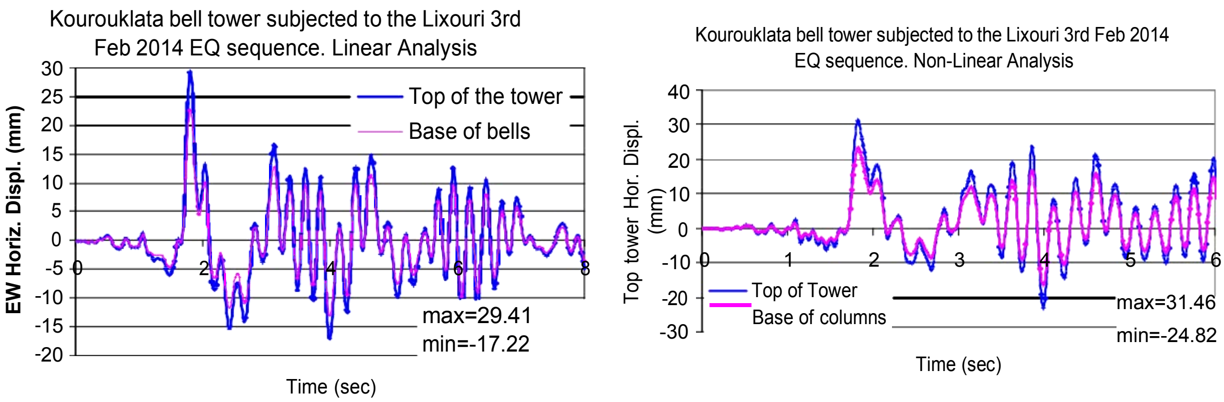

Fig. 18. The horizontal displacement response of the upper part of the Kourouklata bell tower.

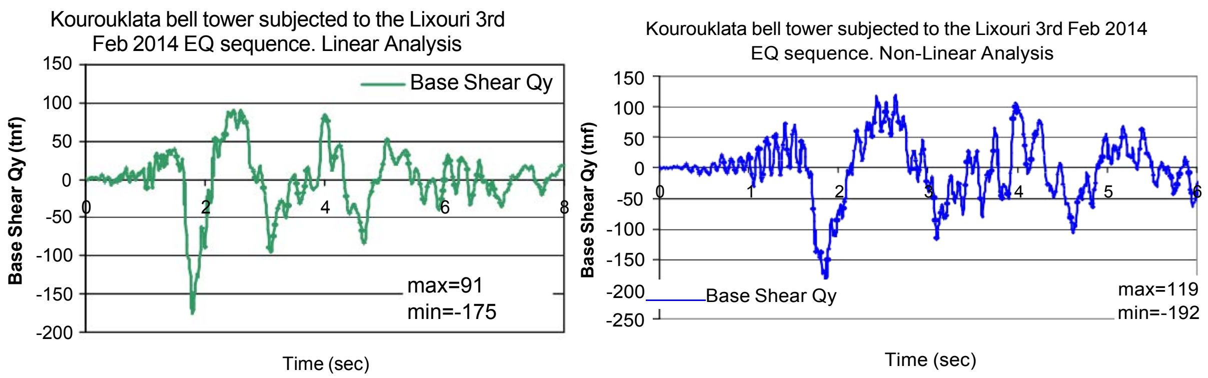

Fig. 19. The Base shear response of the bell tower.

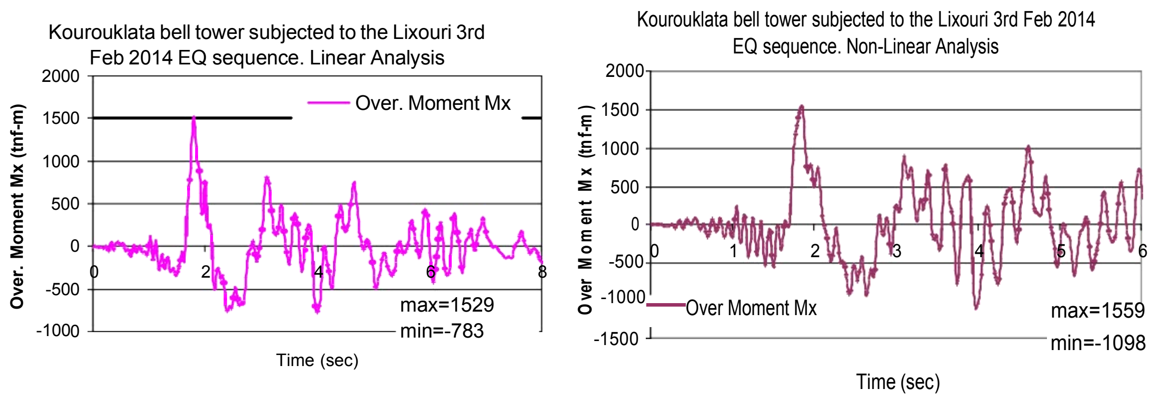

Fig. 20. The Overturning moment response of the bell tower.

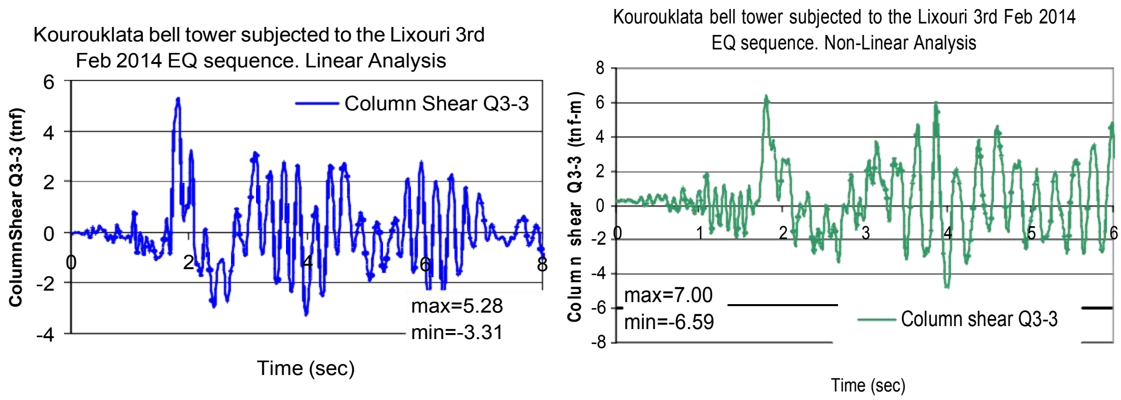

Fig. 21. The column shear response of the upper part of the Kourouklata bell tower.

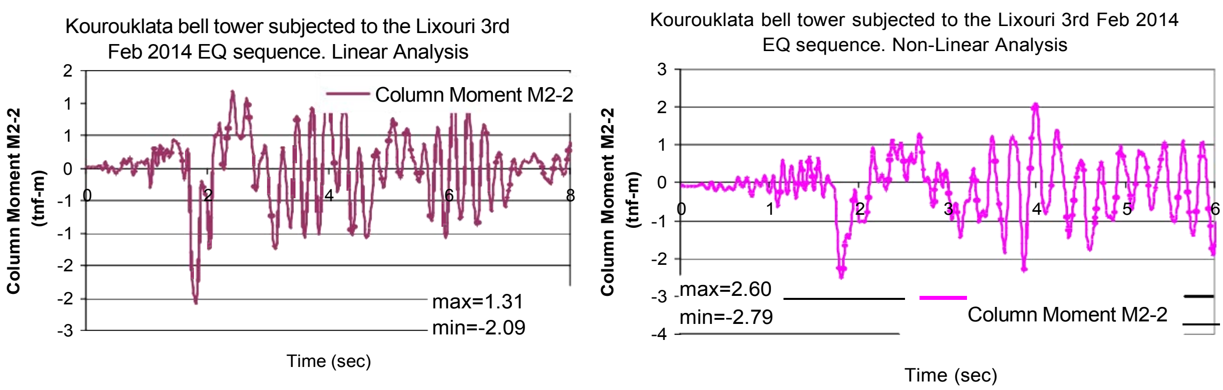

Fig. 22. The column bending moment response of the upper part of the Kourouklata bell tower.

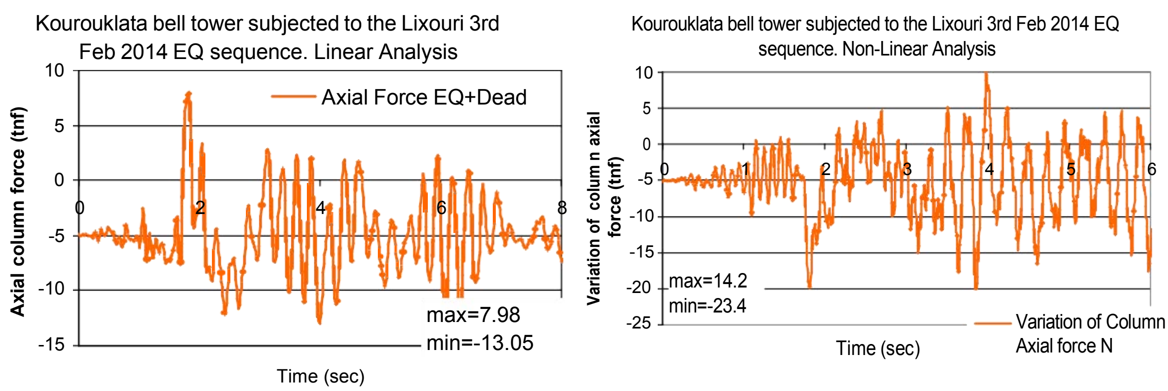

Fig. 23. The column axial force response of the upper part of the Kourouklata bell tower.

In figures 18, 19, 20, 21, 22, 23 the response of the Kourouklata bell tower is shown. At the left hand-side the numerical predictions from the linear time-history analysis are presented whereas at the right hand side the corresponding numerical predictions from the non-linear time-history analysis are also shown. As already mentioned, the non-linear mechanism is confined to the interface between the foundation and the underlying soil layers through the vertical supports having a multi-plastic non-linear behaviour allowing for uplift of the foundation block as well as for a type of hysteretic bahaviour. This is depicted in figure 24 showing the variation o the axial force that develops at two of these vertical supports, one at the South-West and the other at the North-West corner of the foundation block.

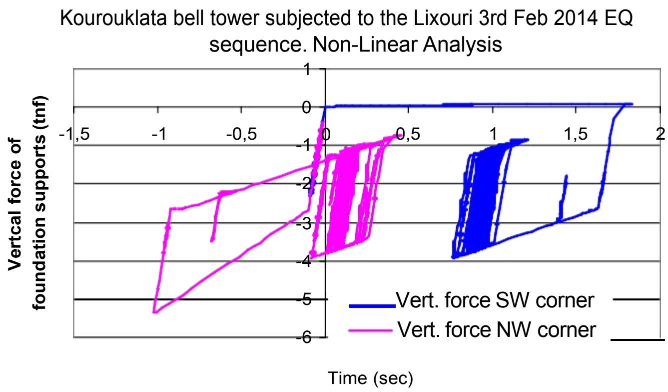

Fig. 24. The variation of the axial force that develops at two vertical supports, one at the South-West and the other at the North-West corner of the foundation block, during the earthquake response of the Kourouklata bell tower subjected to the East-West horizontal of the ground acceleration recorded at Lixouri during the 3rd February 2014 aftershock

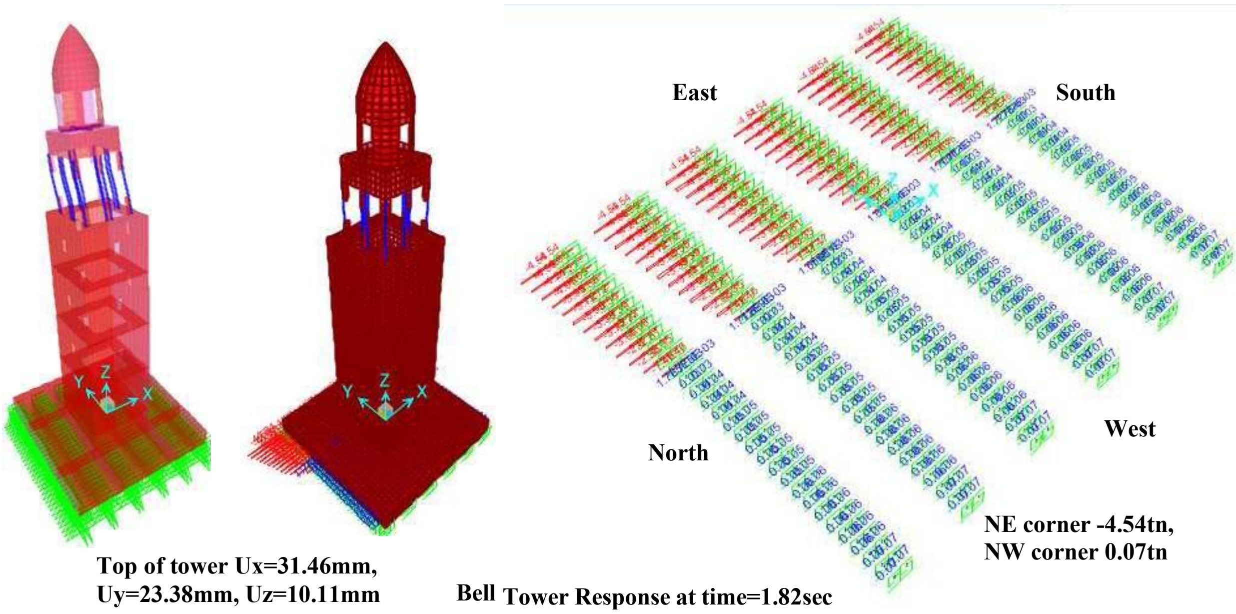

Fig. 25. The horizontal displacement response at the top of the bell tower as well as the axial vertical support forces at the time instant of the time-history East-West sequence (1.82sec) when the base shear force is maximized.

Figure 25 depicts the horizontal displacement response at the top of the bell tower as well as the axial vertical support forces at the time instant of the East-West time-history sequence

(1.82sec) when the horizontal base shear force is maximized. Similarly, figure 26 depicts the stress resultant response of the columns at the top of the bell tower as well as the axial and shear stress response at the bottom of the bell tower again at the time instant of the East-West time-history sequence (1.82sec) when the horizontal base shear force is maximized.

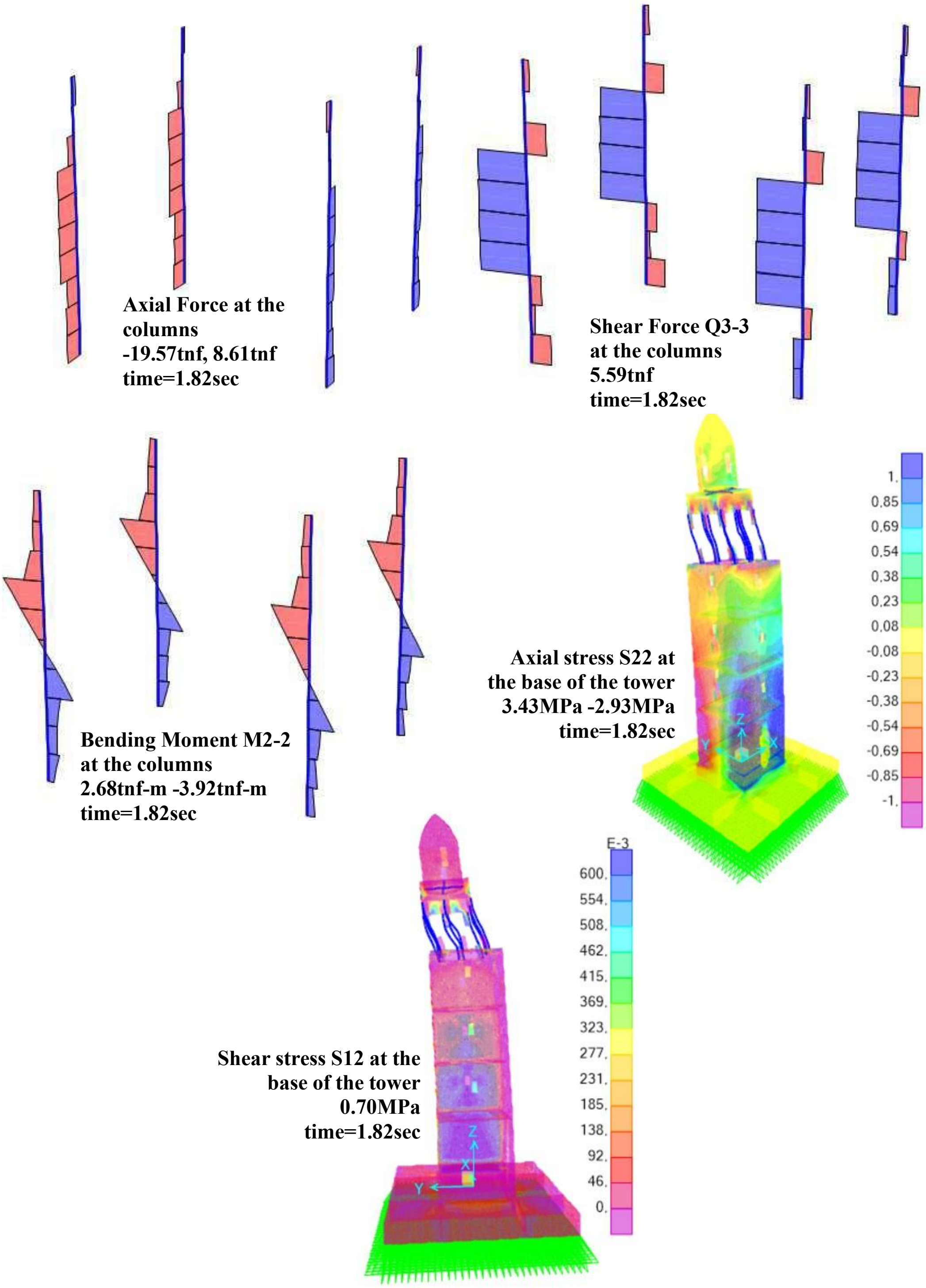

Fig. 26. Stress resultant response at the columns at the top of the bell tower as well as the axial and shear stress response at the bottom of the bell tower at the time instant of the East-West time history sequence (1.82sec) when the base shear force is maximized.

Table 6 lists the peak bell tower earthquake response values predicted by either the linear elastic or the multi-plastic non-linear earthquake dynamic analyses results depicted in figures 13 to 18 as well as in figures 25 and 26. The values listed in this table refer either to the overall earthquake bell tower response in terms of peak horizontal displacements at the tower top or maximum and minimum base shear and overturning moment values (columns 1, 2 and 3). Moreover, the maximum and minimum stress resultants that develop at the columns of the upper part of the bell tower supporting the bells, which sustained the heavy structural damage are also listed (column 4 for the axial force, column 5 for the shear force and column 6 for the bending moment). At the same table, the corresponding shear and flexural capacities are also listed for three different levels of axial force, zero (0KN) compression of 200KN and tension of 100KN, as was in the previous section, whereby the relevant information on the geometry and the reinforcing details were listed together with the assumed mechanical properties for the steel reinforcing bars and the concrete. By comparing the peak overall bell tower response values it can be seen that the values predicted from the non-linear earthquake time history analysis are of the same order of magnitude with those predicted by the linear elastic time history analysis. However, the amplitude of the stress resultants predicted to develop at the columns by the non-linear analysis are more demanding than the ones predicted by the elastic analysis. This must be attributed to the flexibility introduced at the interface between the foundation block and the soil-layers and the frequency content of the excitation resulting in a relatively larger participation of the mass of the upper part of the bell tower in this case than in the linear elastic case, thus resulting in amplified stress resultant values for the columns (original before being strengthened by jacketing) supporting the bells at this upper part.

Table 6. Peak stress resultant earthquake response values for the columns supporting the bells for the Kourouklata bell tower

Dynamic Time History Analyeses based on the East-West horizontal component of the earthquake ground motion recorded at Lixouri	Hor. Disp. Top Tower (mm)	Base Shear (tnf)	Over-turning Moment (tnf-m)	Column Axial Force (KN)	Column Shear Q3-3 (KN)	Column Moment M2-2 (KNm)
	(1)	(2)	(3)	(4)	(5)	(6)
Elastic vertical supports not allowing uplift thus transmitting tensile forces from the foundation to the underlying soil layers. ***Numerically predicted values.***	**29.41** **-17.22**	**91** **-175**	**1529** **-783**	**78.3** **-128**	**51.8** **-32.5**	**12.9** **-20.5**
Multi-plastic vertical supports allowing uplift thus not transmitting tensile forces from the foundation to the underlying soil layers. ***Numerically predicted values.***	**31.46** **-24.82**	**119** **-192**	**1559** **-1098**	**139** **-230**	**68.7** **-64.6**	**25.5** **-27.4**
**** Capacities for axial force 0KN***				**0**	**77**	**38.6**
**** Capacities for axial force 200KN compression***				**-200**	**103**	**60.8**
**** Capacities for axial force 100KN tesnion***				**100**	**64**	**27.3**
***** Capacities for axial force 100KN tension of column strengthen by jacketing. Safety factors concrete 1.5 steel 1.15***				**150**	**140**	**My=78**

* Column cross-section 300mm x 300mm, fc=21.2MPa, 8 rebars 14mm diameter each, fy=240MPa.
** Column cross-section with jacket 350mm x 350mm fc=25MPa, 8 rebars 16mm diameter each, fy=500MPa.

Table 7. Ratio values of demands / capacity for the extreme stress resultant for the columns supporting the bells

Ratios * of demands / capacity values for the extreme stress resultant for the columns supporting the bells	Level of Axial Force	Column Shear Demand Q3-3 / shear capacity	Column Moment Demand M2-2 / flexural capacity
Elastic vertical supports not allowing uplift thus transmitting tensile forces from the foundation to the underlying soil layers. ***Numerically predicted values. Original Column***	**78.3** **-128**	**0.81** **0.32**	**0.47** **0.34**
Multi-plastic vertical supports allowing uplift thus not transmitting tensile forces from the foundation to the underlying soil layers. ***Numerically predicted values. Original column***	**139** **-230**	**1.07 *** **0.63**	**1.0 *** **0.45**
Multi-plastic vertical supports allowing uplift thus not transmitting tensile forces from the foundation to the underlying soil layers. ***Numerically predicted values. Strengthened column by jacketing***	**150**	**0.50**	**0.35**

* Ratio values larger than one indicate structural damage

In table 7 the stress resultant demands in terms of shear force or bending moment (for non-linear numerical predictions) for these columns are compared with the corresponding capacities. As can be seen in this table, for the level of axial force equal or larger than 100KN in tension these shear and flexural capacity values area smaller than the corresponding demand values (the shear and flexure demand over capacity ratio values are equal to 1.07 and 1.0, respectively) thus indicating structural damage. Next, the capacities of a strengthening scheme are also compared with the peak demands predicted through the same multi-plastic non-linear dynamic time-history analysis. The values of the shear and flexural capacities of these strengthened columns are listed at the last row of table together with the most important data for such a strengthening scheme. The ratio values of demand over capacity for either shear or flexure are listed in the last row of table 7. As can be seen these shear and flexure demand over capacity ratio values are equal to 0.50 and 0.35, respectively indicating safe earthquake performance.

6. A RETROFITTING SCHEME UTILIZING A SYSTEM OF VERTICAL PRE-STRESS FORCES.

A non-linear analysis was performed with the bell tower having its foundation block supported on the foundation-soil interface with supports following a multi-plastic constitutive behavior identical to the one depicted previously in figure 17. The push-over horizontal forces are applied at the level 12.88m from the base of the tower. This study focus on the stress filed that is either maximized or minimized at the horizontal level where the bell tower walls are connected to the foundation block. The applied horizontal twin forces (each equal to 75tnf) were assigned a peak total amplitude ±150tnf. Two distinct cases are examined. First, the stress response at the base of the bell tower is depicted without any external intervention whereas in the second case a system of pre-stress forces is applied. These pres-tress forces are applied at the horizontal level of 12.88m with an amplitude of 89tonf at each one of the four corners of the bell tower. The purpose of applying these pre-stress forces was to be able to lower the amplitude of the peak tensile stresses which develop near the base of the bell tower, where it joins the foundation block, due to the overturning mechanism arising from the horizontal seismic actions. In what follows the obtained stress and horizontal displacement results from the case with no pre-stress forces are presented. These results are followed by the corresponding results from the case with the application of the pre-stress forces.

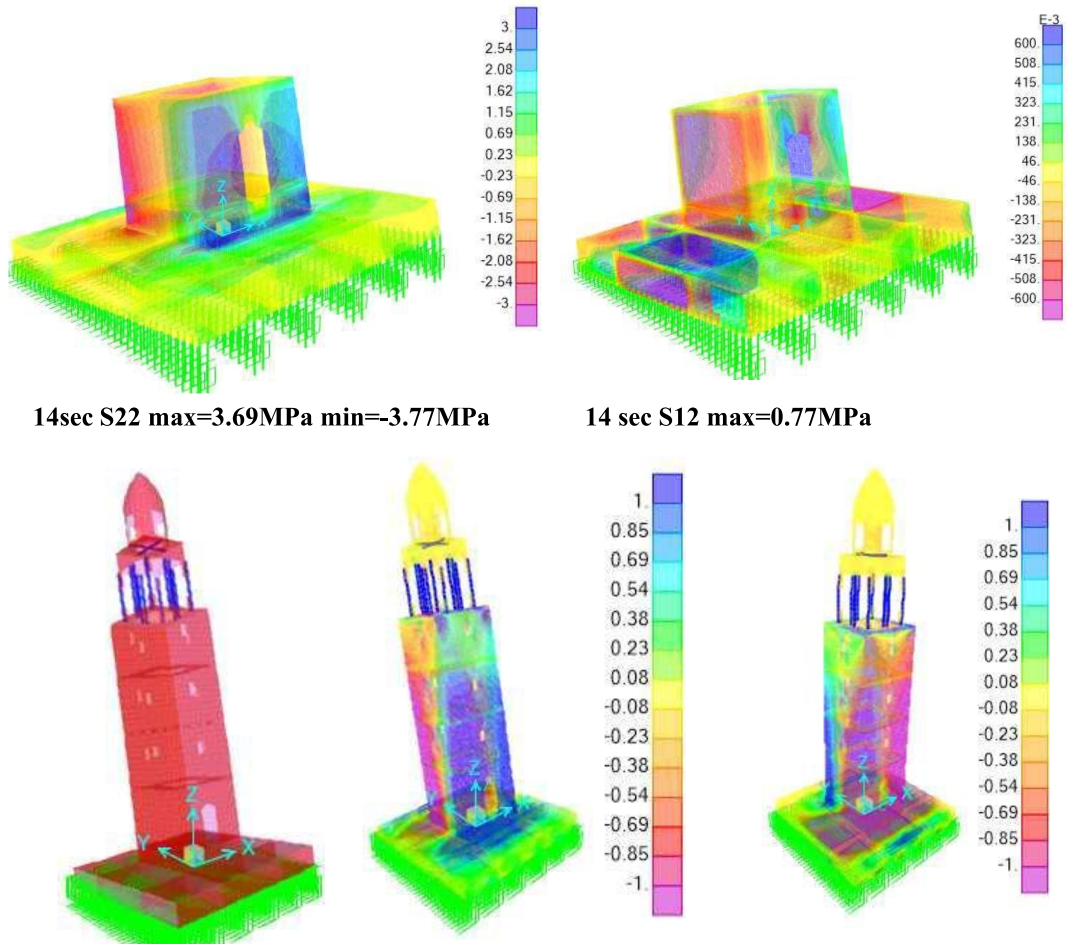

14sec S22 max=3.69MPa min=-3.77MPa **14 sec S12 max=0.77MPa**

Top of tower 14 sec ux=0 uy=162.17mm uz=12.49mm **14sec S22 max=3.69MPa min=-3.77MPa** **14sec S22 max=3.05MPa min=-4.13MPa**

Figure 27. Peak stress and horizontal response of the bell tower from an East-West push-over plus dead load combination at the time when the response is maximized (No pre-stress).

This East-West push over response is plotted for two time instants (14 seconds and 40 seconds) when the bell-tower overturning is reaching peak amplitudes The plotted stress distribution includes the effect of the dead load (plus the pre-stress effect when such forces are present) combined with the stresses resulting from these East-West push-over overturning horizontal forces.

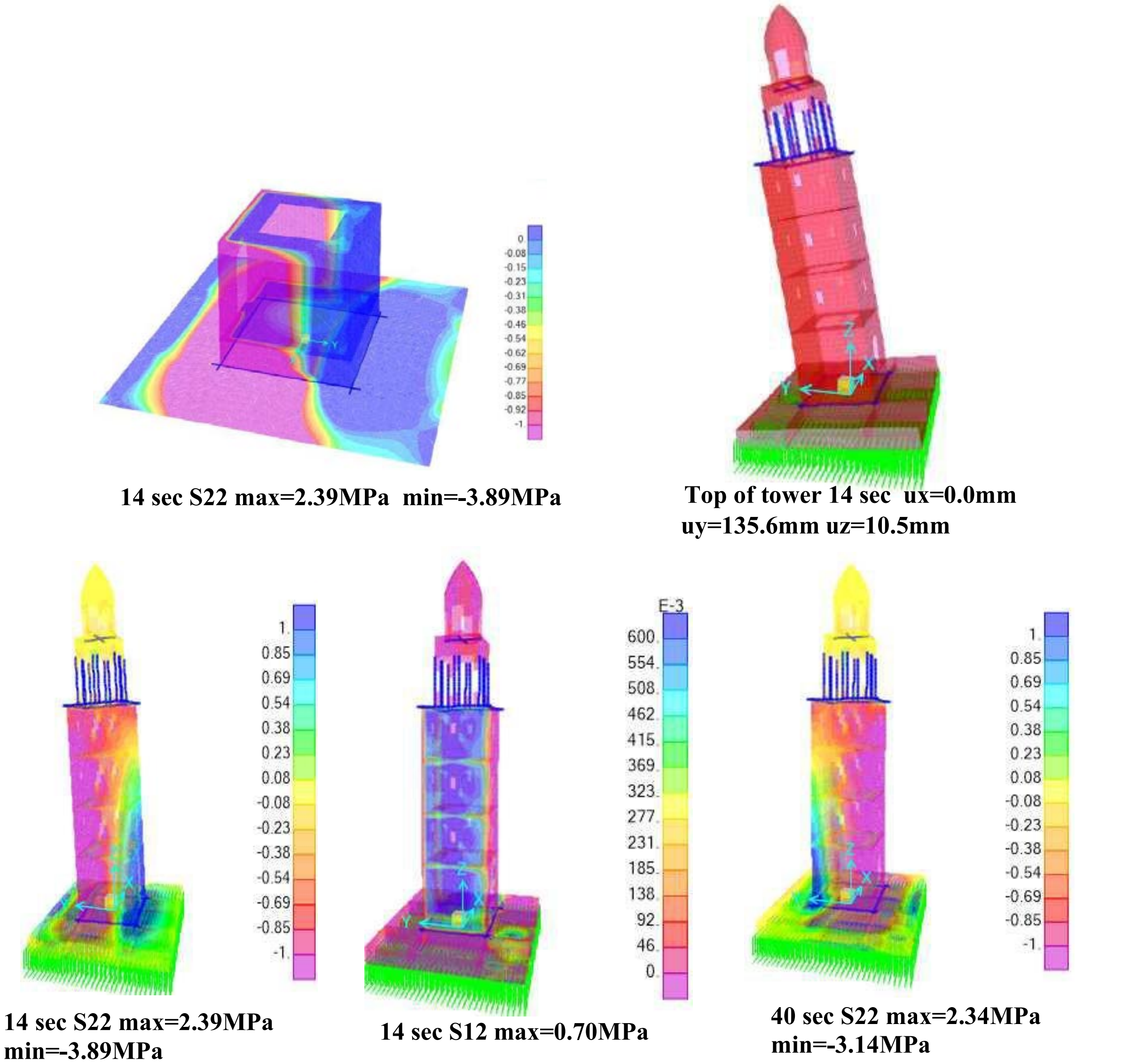

Figure 28. Peak stress and horizontal response of the bell tower from an East-West push-over plus dead + pre-stress load combination at the time when the response is maximized.

From the above figures 27 and 28, by comparing the normal S22 stress response at the base of the bell tower, it can be seen that peak S22 tensile stress is equal to 3.69MPa when no pre-stress forces are applied. The corresponding S22 tensile peak value is equal to 2.39MPa, when the pre-stress forces are applied, signifying a 50% degrease in this tensile stress field. This tensile stress decrease may be beneficial for the seismic performance of a bell tower in the case that the existing reinforcement can not resist effectively such high resulting tensile forces. Due to the anchoring system of the pre-stress forces at the foundation level the foundation block becomes somehow stiffer and this alter to a degree the total displacement response. Figure 29 depicts the variation of Base shear, Over. Moment, horizontal displacement and support forces response of the bell tower from an East-West push-over. Left combined with Dead load + pre-stress forces applied. Left combined only with Dead load (No pre-stress forces).

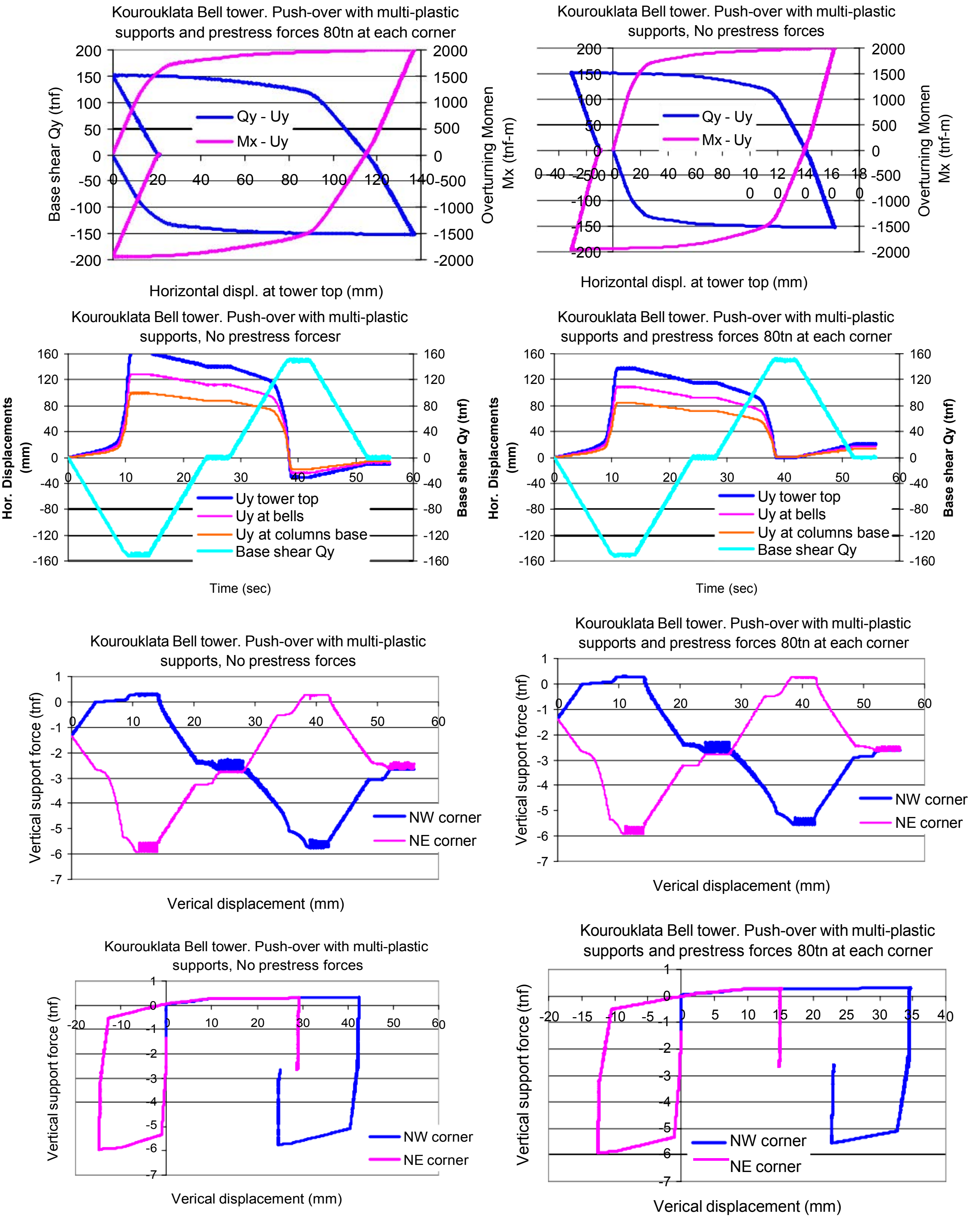

Figure 29. Variation of Base shear, Over. Moment, horizontal displacement and support forces response of the bell tower from an East-West push-over. Left combined with Dead load + pre-stress forces applied. Left combined only with Dead load (No pre-stress forces).

The amplitude of the vertical reactions at the foundation block-soil interface are depicted in figures 30 for the case with no pre-stress forces as well as when pre-stress forces are applied. This vertical force reaction response is shown for three instances. a) When the dead load is fully applied (either with or without pre-stress forces). b) When the East-West push-over force reaches its full amplitude towards the East (14 seconds of the loading sequence) c) When the East-West push-over force reaches its full amplitude towards the West (40 seconds of the loading sequence).

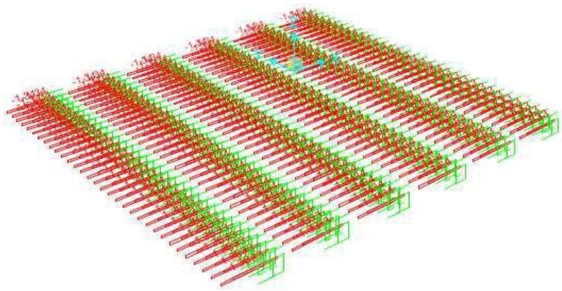

Dead No pre-stress multi plastic
Vertical unit force -1.34tnf

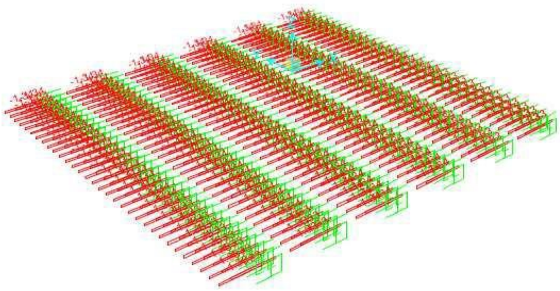

Dead + pre-stress multi plastic
Vertical unit force -1.37tnf

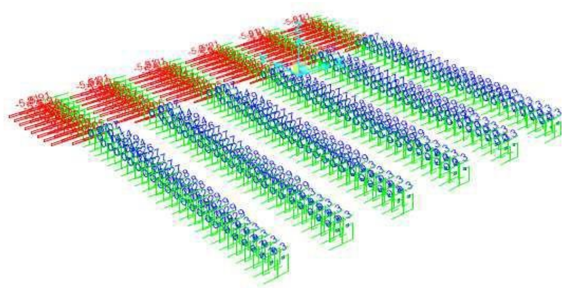

EW Push over No Pre-stress 14 seconds
Vertical unit force -5.91tnf / 0.30tnf

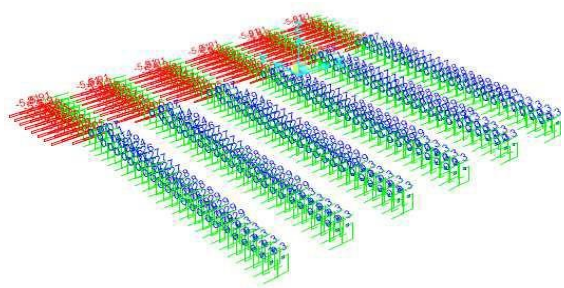

EW Push over + Pre-stress 14 seconds
Vertical unit force -5.87tnf / 0.29tnf

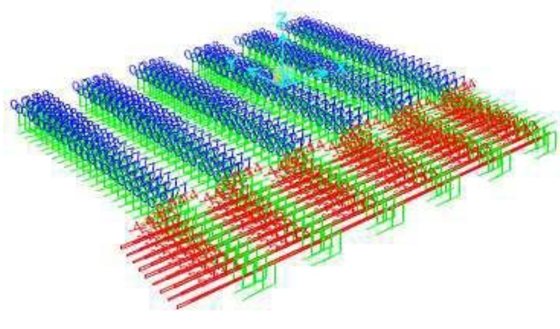

EW Push over No Pre-stress 40 seconds
Vertical unit force -5.71tnf / 0.28tnf

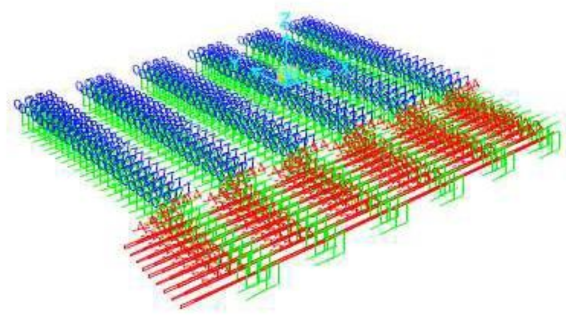

EW Push over + Pre-stress 40 seconds
Vertical unit force -5.47tnf / 0.26tnf

Figure 30. The response of the foundation in terms of the distribution of the vertical reactions of the non-linear links. Response of the bell tower from an East-West push-over. Left combined with Dead load + pre-stress forces applied. Left combined only with Dead load (No pre-stress forces).

Figure 31 depicts the state of axial forces at the pre-stress cables at the end of the pre-stressing process. In tables 8 and 9 the global base shear (Qx and Qy) response quantities for the Havriata and Kourouklata bell towers are listed, respectively. In table 10 the peak force resultants' response for the damage RC columns of the Kourouklata bell tower are also listed.

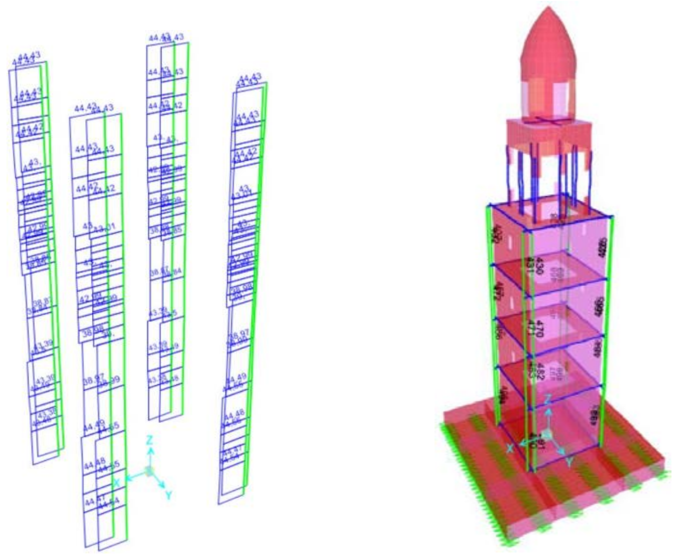

Fig. 31. Distribution of axial forces at the end of pre-stress process 436KN per tendon

Table 8. Base Reactions Havriata

Load case	Base shear Qx kN	Base shear Qy kN
Euro-Code 8 q=3	**688** / **13%**	**688** / **13%**
EW-Con. Duc. μ=3		**1024** / **20%**
NS-Con. Duc. μ=3	**892** / **17%**	
EW + 0.3NS μ=3	**268** / **5.1%**	**1024** / **19.5%**
0.3EW + NS μ=3	**892** / **17%**	**307** / **5.9%**

* The weight of the superstructure (without the foundation block) is 2213kN . The total weight including the foundation block is 5244kN. The percentage of the total weight is indicated

Table 9. Base reactions from the performed numerical analyses for the Kourouklata bell tower

Load case	Base shear Qx kN	Base shear Qy kN
EW-Con. Duc. μ=3		**687** / **13.5%**
NS-Con. Duc. μ=3	**587** / **11.6%**	
EW + 0.3NS μ=3	**177** / **3.5%**	**687** / **13.5%**
0.3EW + NS μ=3	**587** / **11.6%**	**206** / **4.1%**

* The weight of the superstructure (without the foundation block) is 2040kN. The total weight including the foundation block is 5082kN. The percentage of the total weight is indicated

Table 10. Extreme stress resultant for the columns supporting the bells of the Kourouklata

Load case	Axial (KN)	Q2-2 (KN)	Q3-3 (KN)	M2-2 (KNm)	M3-3 (KNm)
DEAD + EW + 0.3NS μ=3	**87 / -184**	**36 / -40**			**24 / -23**
DEAD + 0.3EW + NS μ=3	**97 / -196**		**48 / -52**	**25 / -28**	

Conclusions.

- The 2014 strong earthquake sequence at the island of Kefalonia subjected a number of tall bell towers to considerable seismic forces. Despite the high amplitude of these seismic forces most bell towers in the island did not developed structural damage, with the exception of a bell tower located at the Kourouklata village. This bell tower is the subject of the current special study.
- The fact that the collapsed in 1953 earthquake sequence bell towers were masonry structures whereas the bell towers excited by the 2014 earthquake are reinforced concrete structures can partly explain the observed satisfactory earthquake performance. The studied in this manuscript damaged Kourouklata bell tower revealed that the reinforced concrete structures built in Greece mainly after world war two and the enforcement of the New Code for Seismic Design, e.g. between 1950 and 1996, have a number of weaknesses that can lead to partial or total collapse. These weaknesses have been identified from some time by researchers and professionals specializing in earthquake engineering. Countermeasures for their strengthening are necessary. The effectiveness of such a retrofitting scheme employing pre-stressing cables is numerically studied here. The satisfactory performance of the Havriata bell tower studied previously demonstrates the effectiveness of the current design according to the provisions of the New Greek Seismic Code and Euro-Code8.
- The currently available numerical tools were used to analyze the damage structure and explain the observed earthquake performance. Use is made of the earthquake ground motion of this aftershock recorded during this earthquake sequence. The main objective of this study is to be able through a variety of numerical analyses to yield earthquake response predictions that may partly explain the observed performance.
- Initially, a number of numerical analyses were performed based on linear-elastic response assumptions both for the superstructure as well as with the support conditions of the foundation block on the underlying soil. When these analyses were based on either the Euro-Code 8 design spectra for behaviour factor q=3 or constant ductility (m=3) response spectra derived from the recorded earthquake ground motion the predicted response of the super-structure is in line with the observed performance. However, adopting a constant ductility m=3 value for RC structures that do not develop ductile response should be further discussed. The influence of the structure-foundation-soil interaction is also presented and discussed. This is done by introducing non-linear links at the foundation-soil interface.
- This realistic scenario was studied next employing non-linear mechanisms simulating numerically the possibility of the foundation block to uplift from the underlying soil. This was done in two different ways. First, employing vertical support with multi-linear constitutive behaviour that would allow for a non-linear compressive response but very limited tensile response. Then, the same behaviour was again assumed but adopting at this time a multi-plastic hysteretic behaviour. The obtained numerical non-linear response results in base-shear and overturning values, by either a pushover type of analysis or a time history type of analysis are of the same order of amplitude as the corresponding values based on elastic dynamic spectral analysis employing either the Euro-code 8 design spectra(q=3) or the constant ductility (m=3) response spectra of the recorded earthquake ground motion. The same is also valid for the peak stress levels of the superstructure at critical locations.
- Through this non-linear type of analysis which utilizes vertical supports for the foundation block simulating the uplifting mechanism as well as the hysteretic

behaviour of the soil layers produce stress response predictions which can explain the observed earthquake performance of the studied Kourouklata bell tower. A limit state evaluation of the behaviour of the damaged RC columns was also performed. This was based on the geometry and structural details of the failed columns, on the concrete strength found from destructive laboratory test and on the force resultants that developed on the failed RC columns found from the numerical analyses.

- To the memory of all the Aristotle University students that were killed during the 2023 Tempi-Greece train accident

`REFERENCES

[1] G.C. Manos and E. Kozikopoulos, "In-Situ Measured Dynamic Response of the Bell tower of Agios Gerasimos in Lixouri-Kefalonia, Greece and its Utilization in the Numerical Predictions of its Earthquake Response", *COMPDYN 2015, 5th ECCOMAS Thematic Conference on, Computational Methods in Structural Dynamics and Earthquake Engineering, Crete Island, Greece, 25–27 May 2015.*

[2] George C. Manos and Evaggelos Kozikopoulos "The in-situ measured and computed dynamic response of a bell tower in Kefalonia-Greece", 3rdInternational Conference on Protection of Historical Constructions Lisbon, Portugal, 12 – 15 July, 2017

[3] G.C. Manos, "Study of the Influece of Undelying Soft-soil layers on the Dynamic and Earthquake Response of Bell Towers", COMPDYN 2021, 8th ECCOMAS Thematic Conference on Computational Methods in Structural Dynamics and Earthquake Engineering, M. Papadrakakis, M. Fragiadakis (eds.), Streamed from Athens, Greece, 27–30 June 2021.

[4] G.C. Manos "Seismic Performance of Bell Towers in Kefalonia Greece during the 2014 Earthquake Sequence", COMPDYN 2021, 8th ECCOMAS Thematic Conference on Computational Methods in Structural Dynamics and Earthquake Engineering, M. Papadrakakis, M. Fragiadakis (eds.), Streamed from Athens, Greece, 27–30 June 2021.

[5] George C. Manos "Earthquake Performance of Bell in the Island of Kefalonia, Towers Greece", Journal of Civil Engineering and Architecture 16 (2022) 344-353, doi: 10.17265/1934-7359/2022.07.003.

[6] L. de Stefani, R. Scotta, M. Lazzari, A. Saetta. Seismic improvement of Slender Bell Tower and Minarets. *– PROHITECH, Antalya, Turkey, 2014*

[7] R. M. Azzara, L. Zaccarelli, A. Morelli, T. Trombetti. Seismic Monitoring of the Asinelli and Garisenda Medieval Towers in Bologna (Italy), an Instrumental Contribution to the Engineering Modeling Directed to their Protection. - *PROHITECH, Antalya, Turkey, 2014*

[8] Casolo Siro, Uva Giuseppina. Non-Linear dynamic analysis of masonry towers under natural accelerograms accounting for soil-structure interaction. *– COMPDYN 2013 - Kos Island, Greece, June 12-14, 2013*

[9] A. Saisi, C. Gentile, L. Cantini. Post – Earthquake assessment of a masonry tower by on – site inspection and operational modal testing. *– COMPDYN 2013 - Kos Island, Greece, June 12-14, 2013*

[10] D. Colapieto, A.Fiore, A. Netti, F. Fatiguso, G Marano, M. de Fino D. Cascella, A. Antocona. Dynamic identification and evaluation of the seismic safety of a masonry bell tower in the south Italy. – *COMPDYN 2013 - Kos Island, Greece, June 12-14, 2013*

[11] R. Guidorzi, R. Diversi, L.Vincenzi, C. Mazzotti, V. Simioli. Structural monitoring of the Tower of the Faculty of Engineering in Bologna using MEMS –based sensing. – *EURODYN 2011 – Leuven, Belgium, 4-6 July 2011*

[12] C. Blasi M. Carfagni, S. Carfagni. The use of impulsive actions for the structural identification of Slender monumental buildings- *STREMAH-1991 - Seville, Spain, 14-16 May 1991*

[13] S. Dumorier, W.P. De Wilde. Finite element study of the Tower of Brussels City Hall – *STREMAH 1995 – Chania, Crete, Greece, 1995.*

[14] Manos George, "Consequences on the urban environment in Greece related to the recent intense earthquake activity", *Int. Journal of Civil Engineering and Architecture, Dec. 2011, Volume 5, No. 12 (Serial No. 49), pp. 1065–1090.*

[15] GEER - EERI - ATC - Cephalonia GREECE *Earthquake Reconnaissance January 26th/ February 2nd 2014 Version 1: June 6 2014*

[16] Papaioannou Ch. et al., "Strong ground motion of the 3rd February 2014, (M=6.0) Kefalonia Earthquake", Institute of Earthquake Engineering and Engineering Seismology Report, Feb., 2014.

[17] Papazachos, B. and Papazachou, K., 1989, 1997, 2003. The earthquakes of Greece, *Zitis Publ.,Thessaloniki, 356 pp., 304 pp., 286 pp. (in Greek).*

[18] Provisions of Greek Seismic Code with revisions of seismic zonation", Government Gazette, Δ17α /115/9/ΦΝ275, No. 1154, Athens, 12 Aug. 2003.

[19] Eurocode 8: Design of structures for earthquake resistance - Part 1: General rules, seismic actions and rules for buildings, *FINAL DRAFT prEN 1998-1, December 2003.*

[20] G.C. Manos, et al. (1996) "Predictions of the dynamic characteristics of a 5-story R.C. building at the Volvi Euro-SeisTest Site, utilizing low-intensity vibrations", *3rd European Conference on Structural Dynamics, Eurodyn 1996, Florence, II, 877–884.*

[21] G. C., Manos, V. Kourtides, V.J. Soulis, A.G. Sextos, A. G., and P. Renault, (2006). "Study of the dynamic response of a bridge pier model structure at the Volvi - Greece European Test Site." *8th National Conference on Earthquake Engineering, April 18-22, San Fransisco, U.S.A.*

[22] G.C. Manos, V. Kourtides, A. Sextos, P. Renault, S. Chiras "Study of the dynamic soil-structure interaction of a bridge pier model based on structure and soil measurements" *9th Canadian Conf. on Eartquake Engineering, Ottawa, Ontario, Canada, 26-29 June 2007.*

[23] G.C. Manos, V. Kourtides, A. Sextos, S. Chiras "Soil-Foundation-Bridge Pier Interaction at the Euro-Seis Test Site", *4th Int. Conference on Geotechnical Engineering, Thessaloniki, 24-28 June, 2007.*

[24] G.C. Manos, V. Kourtides, A. Sextos, "Model Bridge Pier Foundation- Soil Interaction implementing, in-situ / shear stack testing and numerical simulation", *14WCEE, Beijing, CHINA, 2008.*

[25] G. C. Manos , K.D. Pitilakis, A.G. Sextos, V. Kourtides, V. Soulis, J. Thauampteh, “Field experiments for monitoring the dynamic soil-structure-foundation response of model structures at a Test Site” *Journal of Structural Engineering, American Society of Civil Engineers, Special Issue “Field Testing of Bridges and Buildings, D4014012, Vol. 141, Issue 1, January 2015.*

[26] George C. Manos, Lambros Kotoulas and Evangelos Kozikopoulos “Evaluation of the Performance of Unreinforced Stone Masonry Greek “Basilica” Churches When Subjected to Seismic Forces and Foundation Settlement”, Buildings 2019, 9, 106; doi:10.3390/buildings9050106.